

Search for Excited States in ${}^3\text{He}^\dagger$

K. H. Bray,* S. N. Bunker, Mahavir Jain, K. S. Jayaraman, G. A. Moss,* W. T. H. van Oers,
D. O. Wells, and Y. I. Wu

Cyclotron Laboratory and Department of Physics, University of Manitoba, Winnipeg 19, Canada

(Received 30 November 1970)

A search has been made for excited states in ${}^3\text{He}$ by investigating proton-induced reactions on ${}^6\text{Li}$. The investigation consisted of two parts. In the first part, a kinematically incomplete experiment, the ${}^3\text{He}$ and α -particle continua from the ${}^6\text{Li}(p, {}^3\text{He})$ and ${}^6\text{Li}(p, \alpha)$ reactions at an incident proton energy of 45.0 MeV have been studied for structure due to excited states in ${}^4\text{He}$ and ${}^3\text{He}$, respectively. The ${}^3\text{He}$ and α -particle spectra were measured from 15 to 90° (lab) in steps of 5° using a ΔE - E detector telescope. The ${}^3\text{He}$ spectra exhibit clearly discernible peaks due to the 20.2-MeV (0^+ , $T=0$) and 21.4-MeV (0^- , $T=0$) excited states in ${}^4\text{He}$. In the α -particle spectra no structure has been observed that could be interpreted as due to excited states in ${}^3\text{He}$ for excitation energies up to 17.5 MeV. An upper limit of 30 $\mu\text{b}/\text{sr}$ could be set for the excitation of states in ${}^3\text{He}$ having a width $\lesssim 1.0$ MeV. In the second part, a kinematically complete experiment, a study has been made of the ${}^6\text{Li}(p, \alpha d)p$ reaction at an incident proton energy of 45.0 MeV. This investigation was carried out to study final-state interactions and, in particular, to search for a possible p - d final-state interaction corresponding to a resonance in ${}^3\text{He}$. Coincidence spectra from the ${}^6\text{Li}(p, \alpha d)p$ reaction were measured in coplanar geometry with the α -particle detector set at 50° (lab), while the deuteron-detector telescope was moved in steps of 10° from -100 to -50° (lab), and with the α -particle detector set at 30° (lab) and the deuteron-detector telescope at -100 and -80° (lab). The measured coincidence spectra show a prominent p - α final-state interaction corresponding to the ground state of ${}^5\text{Li}$. No other strong p - α final-state interaction was observed. The coincidence spectra do not exhibit a p - d final-state interaction corresponding to a $T=\frac{1}{2}$ resonance in ${}^3\text{He}$ of excitation between 5.5 and 20 MeV.

I. INTRODUCTION

Recently there has been considerable interest in the possible existence of virtual states and/or resonances in the three-nucleon system. The experimental and theoretical investigations received strong impetus after Ajdacić *et al.*¹ reported on the evidence for the existence of a trineutron bound by about 1 MeV in the reaction ${}^3\text{H}(n, p)3n$ at 14.4 MeV. Shortly thereafter, Kim *et al.*² reported on a study of the ${}^3\text{He}(p, p')$ reaction at 30.2 MeV in which they found evidence for three states in ${}^3\text{He}$ with excitation energies of 8.2, 10.2, and 12.6 MeV having widths of about 0.9 MeV. The same group also found evidence for the latter two excited states in ${}^3\text{He}$ in a study of the ${}^6\text{Li}(p, \alpha)$ reaction,³ again at an incident proton energy of 30.2 MeV. The experiments just mentioned have been repeated with negative results by various experimental groups. In addition a great number of other reactions have been examined for structure which could be related to excited states in the three-nucleon system (see Table I). More recently Williams *et al.*⁴ measured continuum neutron spectra from the ${}^3\text{H}(p, n)$ and ${}^3\text{He}(p, n)$ reactions at 30 and 50 MeV. The structure in these spectra was interpreted as due to broad resonances in the three-nucleon system. The observed excitation energies (with respect to the ground state of ${}^3\text{He}$)

and widths are $E_x=9.6\pm 0.7$, $\Gamma=5\pm 1$ MeV, and $E_x=16\pm 1$, $\Gamma=9\pm 1$ MeV, respectively. The isospin values which were assigned are $T=\frac{1}{2}$ for the first resonance and $T=\frac{3}{2}$ for the second one. Supporting evidence for a broad $T=\frac{3}{2}$ resonance in the three-nucleon system comes also from a study of the ${}^3\text{He}(\pi^-, \pi^+)3n$ double-charge-exchange reaction by Sperinde *et al.*⁵ This reaction showed a resonant behavior in the three-neutron system within a few MeV of threshold ($E_x=2$, $\Gamma=12$ MeV). It is interesting to note that earlier Ohlsen, Stokes, and Young⁶ claimed to have found some evidence for such a resonance at 1 to 1.5 MeV above threshold in a study of the reaction ${}^3\text{H}(t, {}^3\text{He})3n$ at 22.3 MeV.

In a discussion about possible excited states of the three-nucleon system a distinction should be made between virtual states and resonant states. If the three-nucleon system is thought to be composed of a single nucleon c and a two-nucleon system d , then virtual and resonant states differ decidedly in the nature of the energy dependence of the phase shifts for c - d scattering.⁷ A virtual state is characterized by a strong increase in the cross section for c - d scattering for decreasing energy caused by an attractive interaction not quite strong enough to form a bound state of the c - d system. Resonant states of the c - d system are excited states unstable against decay into

TABLE I. Experimental evidence concerning a possible excited state of the three-nucleon system.

Reaction	Incident energy (MeV)	Angular range (deg)	Cross section (mb/sr)	Remarks	Reference
${}^3\text{H}(n, p){}^3\text{He}$	14.4	5-20	$d\sigma/d\Omega(5^\circ) = 12 \pm 5$ integrated from $E_{pL} = 2.7$ to 6.1 MeV	Evidence for trineutron	1
${}^3\text{H}(n, p){}^3\text{He}$	14.1, 18.2, 21.5			No evidence for trineutron	a
${}^3\text{H}(n, p){}^3\text{He}$	15.2	0, 15	$d\sigma/d\Omega(0^\circ) = 25 \pm 6$, $d\sigma/d\Omega(15^\circ) = 10 \pm 3$, integrated from $E_{pL} = 3.5$ to 6.0 MeV	No evidence for trineutron	b
${}^3\text{H}(n, p){}^3\text{He}$	20.8	0	$d\sigma/d\Omega(0^\circ) = 3.5 \pm 2.0$ integrated from $E_{pL} = 6.5$ to 14.4 MeV	No evidence for trineutron	c
${}^3\text{H}(t, {}^3\text{He}){}^3\text{He}$	22.25	8-20		Weak evidence for a trineutron unbound by 1-1.5 MeV	6
${}^3\text{He}(\pi^-, \pi^+){}^3\text{He}$	140	15-40		Evidence for a broad resonance in ${}^3\text{He}$ system ($E_x = 2$, $\Gamma = 12$ MeV)	5
${}^7\text{Li}(n, {}^3\text{He}){}^5\text{Li}$	14-19			No evidence for bound trineutron	d
${}^3\text{He}(n, p)np$	14.4	5	$\sigma_{\text{tot}} \leq 1$ mb $d\sigma/d\Omega(5^\circ) = 2 \pm 1$ integrated from $E_{pL} = 2.7$ to 6.1 MeV	No evidence for three-nucleon final-state interaction	e
${}^3\text{He}(t, {}^3\text{He}){}^3\text{H}^*$	22.5	8-20		No evidence for ${}^3\text{H}^*$	6
${}^6\text{Li}(\pi^-, t){}^3\text{H}^*$	π^- capture			No evidence for ${}^3\text{H}^*$	f
${}^3\text{He}(p, p'){}^3\text{He}^*$	25.0	25, 35, 50	Upper limit = 0.25	No evidence for ${}^3\text{He}^*$, $3 < E_x < 15$ MeV	g
${}^3\text{He}(p, p'){}^3\text{He}^*$	25.5	11-70	Upper limit = 0.3 \pm 0.1	No evidence for ${}^3\text{He}^*$, $E_x < 12$ MeV	h
${}^3\text{He}(p, p'){}^3\text{He}^*$	30.2	10-40	$d\sigma/d\Omega(15^\circ) = 2$ ($E_x = 10.2$ MeV)	Evidence for ${}^3\text{He}^*$, $E_x = 8.2, 10.2$ ($\Gamma = 0.9$ MeV), and 12.6 MeV ($\Gamma = 0.9$ MeV)	2
${}^3\text{He}(p, p'){}^3\text{He}^*$	30.6	17, 20, 26	Upper limit = 0.15 with $\Gamma \approx 1.0$ MeV	No evidence for ${}^3\text{He}^*$	i
${}^3\text{He}(p, p'){}^3\text{He}^*$	30.9	15, 26	Upper limit (26^\circ) = 0.25 with $\Gamma \approx 1.0$ MeV	No evidence for ${}^3\text{He}^*$	j

TABLE I (Continued)

Reaction	Incident energy (MeV)	Angular range (deg)	Cross section (mb/sr)	Remarks	Reference
${}^3\text{He}(p, p'){}^3\text{He}^*$	34.2	17.5 25.0	Upper limit=0.6 Upper limit=0.3 with $\Gamma = 1.0$ MeV	No evidence for ${}^3\text{He}^*$	k
${}^3\text{He}({}^3\text{He}, {}^3\text{He}'){}^3\text{He}^*$	44, 53	5-42	Upper limit=0.12	No evidence for ${}^3\text{He}^*$, $E_x < 30$ MeV	l
${}^3\text{He}(\alpha, \alpha'){}^3\text{He}^*$	42	17.5, 20.0 22.0, 25.0	Upper limits 0.2, 0.4, 0.2, 0.15 with $\Gamma = 1.0$ MeV	No evidence for ${}^3\text{He}^*$	m
${}^3\text{He}(e, e'){}^3\text{He}^*$	200	60	Upper limit $= 3 \times 10^{-33}$ cm ² /sr	No evidence for ${}^3\text{He}^*$, $5.5 < E_x < 17$ MeV	n
${}^3\text{H}(p, n){}^3\text{He}^*$	30.3 49.5	10-30 2-60		Evidence for broad resonances in ${}^3\text{He}$ system at 16 MeV ($\Gamma = 9$ MeV) and 9.6 MeV ($\Gamma = 5$ MeV)	4
${}^6\text{Li}(p, \alpha){}^3\text{He}^*$	20.0	15-85	Upper limit (20) $= 0.3$ with $\Gamma = 0.9$ MeV	No evidence for ${}^3\text{He}^*$ ($T = \frac{1}{2}$)	23
${}^6\text{Li}(p, \alpha){}^3\text{He}^*$	30.2	10-40		Evidence for ${}^3\text{He}^*$, $E_x = 10.2, 12.6$ MeV	3
${}^6\text{Li}(p, \alpha){}^3\text{He}^*$	45.0	15-90	Upper limit (25) $= 0.03$ with $\Gamma \approx 0.5$ MeV	No evidence for ${}^3\text{He}^*$ ($T = \frac{1}{2}$)	Present work
${}^2\text{H}(p, p){}^3\text{H}$	3-9			No evidence for ${}^3\text{He}^*$ ($T = \frac{1}{2}$)	o
${}^2\text{H}(p, d^*)p$	9-13	30, 77 80	Excitation function for d^* production	Evidence for ${}^3\text{He}^*$ ($E_x = 12.4$ MeV)	p
${}^2\text{H}(p, d^*)p$	7-17	25	Excitation function for d^* production	Possible evidence for ${}^3\text{He}^*$ ($E_x = 12.4$ MeV) or threshold effect	q
$p + {}^6\text{Li} \rightarrow p + d + \alpha$ all possible two-particles coincidences	9, 10			No evidence for $p-d$ final-state interaction, $5.5 < E_x < 12.5$ MeV	24
${}^6\text{Li}(p, \alpha d)p$	45.0	$\theta_\alpha = 50$ $50 \leq \theta_d \leq 100$ $\theta_\alpha = 30, \theta_d = 80, 100$		No evidence for $p-d$ final-state interaction, $5.5 < E_x < 20$ MeV	Present work

TABLE I (Continued)

Reaction	Incident energy (MeV)	Angular range (deg)	Cross section (mb/sr)	Remarks	Reference
${}^3\text{He}(p,n){}^3\text{p}$	13.1	20	$d\sigma/d\Omega(20^\circ) = 0.005 \pm 0.018$, integrated from $E_{nL} = 1.7$ – 4.1 MeV	No evidence for three-nucleon final-state interaction	r
${}^3\text{He}(p,n){}^3\text{p}$	14.1	3–80	Upper limit $d\sigma/d\Omega(\theta) = 0.5 \pm 0.3$ integrated from $E_{nL} = 3.0$ to 5.85 MeV	No evidence for three-nucleon final-state interaction	s
${}^3\text{He}(p,n){}^3\text{p}$	30.3, 49.5	10–30 2–50		Evidence for a broad resonance in ${}^3\text{p}$ system at 9 MeV ($\Gamma = 10.5$ MeV)	4
${}^3\text{He}(p,n){}^3\text{p}$	24.9	8		Deviation from four-body phase space prediction	t
${}^3\text{He}(p,n){}^3\text{p}$	44	6–25		No evidence for three-nucleon final-state interaction	u
${}^6\text{Li}({}^3\text{He}, {}^6\text{He}){}^3\text{p}$	53.2	14.1		No evidence for three-nucleon final-state interaction	v

^aK. Debertin and E. Rössle, Nucl. Phys. A107, 693 (1967).

^bE. Fuschini, C. Maroni, A. Uquzzoni, E. Verondini, and A. Vitale, Nuovo Cimento 48B, 190 (1967).

^cS. T. Thornton, J. K. Bair, C. M. Jones, and H. B. Willard, Phys. Rev. Letters 17, 701 (1966).

^dK. Fujikawa and H. Morinaga, Nucl. Phys. A115, 1 (1968).

^eB. Antolković, M. Cerineo, G. Paif, P. Tomas, V. Ajdacić, B. Lalović, W. T. H. van Oers, and I. Šlaus, Phys. Letters 23, 477 (1966).

^fR. C. Minehart, L. Coulson, W. F. Grubb, III, and K. Zioc, Phys. Rev. 177, 1464 (1969).

^gS. M. Austin, W. Benenson, and R. A. Paddock, Bull. Am. Phys. Soc. 12, 16 (1967).

^hJ. Cerny, C. Detraz, H. Pugh, and I. Šlaus, unpublished.

ⁱS. A. Harbison, F. G. Kingston, A. R. Johnston, and E. A. McClatchie, Nucl. Phys. A108, 478 (1968).

^jM. D. Mancusi, C. M. Jones, and J. B. Ball, Phys. Rev. Letters 19, 1449 (1967).

^kE. Bar-Avraham, R. F. Carlson, C. C. Chang, H. H. Forster, C. C. Kim, J. R. Richardson, I. Šlaus, P. Tomas, W. T. H. van Oers, and J. W. Verba, in *Proceedings of the International Conference on Nuclear Structure*, edited by J. Sanada (supplement to J. Phys. Soc. Japan, Tokyo, 1969), p. 80.

¹R. J. Slobodrian, J. S. C. McKee, D. J. Clark, W. F. Tivol, and T. A. Tombrello, Nucl. Phys. A101, 109 (1967).

^mR. E. Warner, J. S. Vincent, and E. T. Boschitz, Phys. Letters 24B, 91 (1967).

ⁿR. F. Frosch, H. Crannell, J. S. McCarthy, R. E. Rand, R. S. Safrata, L. R. Suelzle, and M. R. Yearian, Phys. Letters 24B, 54 (1967).

^oD. Daronian, J. S. Faivre, D. Garreta, J. Goudergues, J. Jungerman, H. Krug, B. Mayer, A. Pages, A. Papineau, and J. Testoni, Nucl. Phys. A104, 111 (1967).

^pA. Miller, W. von Witsch, G. C. Phillips, C. Joseph, and V. Valković, Phys. Rev. C 1, 1342 (1970).

^qJ. C. van der Weerd, T. R. Canada, C. L. Fink, and B. L. Cohen, Phys. Rev. C 3, 66 (1971).

^rJ. A. Cookson, Phys. Letters 22, 612 (1966).

^sJ. D. Anderson, C. Wong, J. W. McClure, and B. A. Pohl, Phys. Rev. Letters 15, 66 (1965).

^tA. D. Bacher, F. G. Resmini, R. J. Slobodrian, R. de Swinarski, H. Meiner, and W. M. Tivol, Phys. Letters 29B, 573 (1969).

^uT. A. Tombrello and R. J. Slobodrian, Nucl. Phys. A111, 236 (1968).

^vA. D. Bacher, R. L. McGrath, J. Cerny, R. de Swinarski, J. C. Hardy, and R. J. Slobodrian (private communication).

particles c and d . For a virtual state one expresses the scattering phase shift δ analogous to the nucleon-nucleon system, in terms of the scattering length a and effective range r_0 , by

$$k \cot \delta = -\frac{1}{a} + \frac{1}{2} r_0 k^2,$$

where k is the wave number for the relative motion of the c - d pair. For the nucleon-deuteron system, neglecting Coulomb effects, an effective-range expansion of this form can only be applied to s -wave scattering in the spin state with total spin $\frac{3}{2}$ (4S state). It has been shown⁸ that for s -wave scattering in the spin state with total spin $\frac{1}{2}$ (2S state) the scattering phase shift should be expressed as

$$k \cot \delta = A/(1+Bk^2) + C + Dk^2,$$

due to the existence of a pole at a negative energy [$E = -(\hbar^2/2\mu)(1/B)$].

The phase shift for resonance scattering can be written

$$\delta = \delta_0 + \tan^{-1}[\Gamma/(E_0 - E)],$$

where E_0 and Γ are the energy and the width of the resonance, E is the energy of the relative motion of the c - d pair, and δ_0 is the phase shift for potential scattering. According to Baz', Gol'danskii, and Zel'dovich,⁷ the lifetime of excited states of the c - d system can be expressed in terms of the scattering phase shift δ by

$$\tau(E) = (2\mu/\hbar k)(R + d\delta/dk),$$

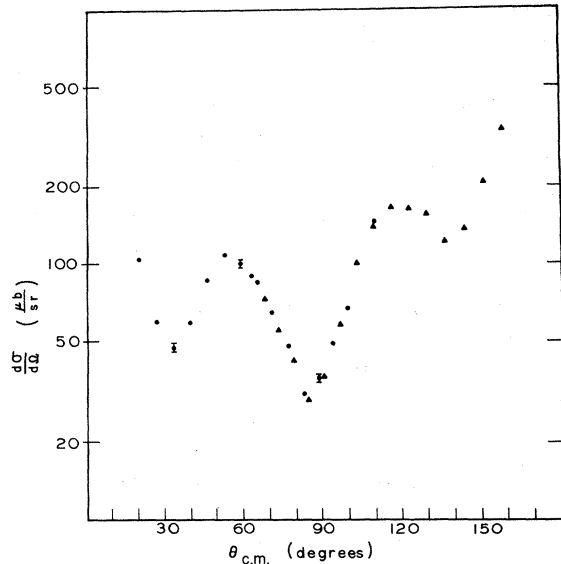


FIG. 1. Center-of-mass angular distribution for the ${}^6\text{Li}(p, {}^3\text{He}){}^4\text{He}(g.s.)$ reaction at 45.0 MeV. The circles and triangles indicate whether the observed particle was a ${}^3\text{He}$ particle or an α particle.

where μ denotes the reduced mass of the c - d system and R is a reasonable approximation to the range of interaction. As pointed out by Wigner,⁹ causality imposes a lower limit on the derivative of the scattering phase shift with energy; i.e., $d\delta/dk > -R$. Consequently, for virtual 4S states one obtains for the lifetime in the limit of small energies $|a|k \ll 1$:

$$\tau \approx (2\mu/\hbar k)(R - a).$$

Similarly, for virtual 2S states one gets for the lifetime, again in the limit of small energies,

$$\tau \approx (2\mu/\hbar k)[R + 1/(A + C)].$$

In order for an excited state to have a definite physical meaning, its lifetime should be much greater than the transit time of the incident particle through the region of interaction. Thus, for the case of a relatively long-lived virtual state of the intermediate nucleus, one must have $-a \gg R$. For $R = 3$ F the condition is $-a \gg 3$ F. Furthermore, such a long-lived virtual state can only be formed for small relative energies of the interacting particles: $k \ll 1/|a|$, or for the nucleon-deuteron system ($E \ll 4$ MeV for $k \ll \frac{1}{3}$ F⁻¹).

The experimental values^{8,10} for the neutron-deuteron scattering lengths are ${}^4a_{n-d} = 6.11 \pm 0.06$ F and ${}^2a_{n-d} = -1/(A + C) = 0.12 \pm 0.07$ F. The values for the proton-deuteron scattering lengths, which can be deduced only from a phase-shift analysis of p - d elastic scattering, are ${}^4a_{p-d} = 11.9^{+0.3}_{-0.3}$ F and ${}^2a_{p-d} = 1.0 \pm 0.5$ F. The other parameters of the effective-range expansions are discussed in Ref. 8. From these values one can conclude that low-energy nucleon-deuteron scattering is predominantly determined by the 4S amplitudes. Thus, the anomalous behavior of $k \cot \delta$ for the 2S state does not lead to a pronounced threshold effect. Experimentally it has been demonstrated^{11,12} that a strong 4S nucleon-deuteron final-state interaction is not observed.

For scattering through a resonance, the lifetime of the intermediate nucleus is given by

$$\tau(E) \approx \frac{2\mu R}{\hbar k} + \frac{2\hbar}{\Gamma} \frac{\Gamma^2}{(E - E_0)^2 + \Gamma^2}.$$

It is assumed that the nonresonant part of the phase shift (δ_0) changes only slowly with energy and thus $d\delta_0/dk \approx 0$. Choosing $E = E_0$, one gets

$$\tau(E_0) \approx 2\mu R/\hbar k + 2\hbar/\Gamma.$$

Similar reasoning gives the condition $\hbar/\Gamma \gg \mu R/\hbar k$ for the existence of a resonant state. Accordingly, for excitation energies in ${}^3\text{He}$ up to 20 MeV, the width Γ of the resonant state should satisfy the condition $\Gamma \ll 13$ MeV. Therefore the $T = \frac{3}{2}$ resonances with widths $\Gamma \approx 10$ MeV, for which evidence

has been claimed by Williams *et al.*⁴ and Sperinde *et al.*,⁵ poorly fit the condition given above. Similar remarks apply to the $T = \frac{1}{2}$ resonance observed by Williams *et al.*⁴

The present experiment was designed to look for relatively narrow ($\Gamma \lesssim 1$ MeV) $T = \frac{1}{2}$ excited states in ${}^3\text{He}$. In particular, it was felt desirable to extend the range of excitation energies in ${}^3\text{He}$ to higher energies than previously studied. The investigation consisted of two parts. In the first, a kinematically incomplete experiment, a study has been made of the ${}^6\text{Li}(p, {}^3\text{He})$ and ${}^6\text{Li}(p, \alpha)$ reactions at an incident proton energy of 45.0 MeV. The ${}^3\text{He}$ - and α -particle continua were examined for structure which could be interpreted as due to excited states in ${}^4\text{He}$ and ${}^3\text{He}$, respectively. The experimental details are given in Sec. II A, while the results are discussed in Sec. II B. In the second part of the investigation a study has been made of the ${}^6\text{Li}(p, \alpha d)p$ reaction at an incident proton energy of 45.0 MeV in a kinematically complete ex-

periment. Here a search was made for a possible proton-deuteron final-state interaction which would correspond to a $T = \frac{1}{2}$ resonance in ${}^3\text{He}$. The experimental details are given in Sec. III A, while the results are discussed in Sec. III B. Finally, Sec. IV contains concluding remarks.

II. KINEMATICALLY INCOMPLETE EXPERIMENT ${}^6\text{Li}(p, \alpha)$

A. Experimental Arrangements and Procedure

A momentum-analyzed proton beam from the University of Manitoba sector-focused cyclotron was used to bombard self-supporting targets enriched in ${}^6\text{Li}$ to 99.6% and with thicknesses in the range of 1–3 mg cm⁻². The incident proton beam had an energy of 45.0 ± 0.15 MeV, while its energy spread was estimated to be 200-keV full width at half maximum (FWHM). A description of the scattering chamber has been given previously.¹³ The lithium targets were prepared using an evaporation method. The target thicknesses were determined by weighing and by energy-loss measurements of α particles from ${}^{241}\text{Am}$ and ThC sources.

The reaction products were observed with a ΔE - E detector telescope consisting of a 100- μ -thick surface-barrier detector (ΔE), and a 3-mm-thick lithium-drifted silicon detector (E). A solid-angle-defining collimator (copper, 0.156 in. thick), with an aperture 0.125 in. wide by 0.313 in. high, was placed in front of the detector telescope at a distance of 12.00 in. from the scattering-chamber center. An antiscattering baffle was located halfway between the solid-angle-defining collimator and the scattering-chamber center. Spectra for ${}^3\text{He}$ and α particles were observed from 15 to 90° (lab) in steps of 5° using, in conjunction with the detector telescope, a particle identifier and conventional electronics. The analog pulses corresponding to ${}^3\text{He}$ and α particles were fed into the analog to digital converters (ADC's) of a Nuclear Data pulse-height analyzer and of a PDP-9 computer, respectively.

As discussed previously,¹³ no collimation of the incident beam was done after the energy-analyzing slits in the vault area. To monitor the direction of the beam incident on the target, two monitor counters with identical geometry were utilized. The proton beam was collected in a Faraday cup and integrated using a current integrator.

B. Results and Discussion

The observed ${}^3\text{He}$ - and α -particle spectra show, besides broad continua, a number of peaks of which the most prominent is the particle group from the ${}^6\text{Li}(p, {}^3\text{He}){}^4\text{He}$ (g.s.) reaction. The center-

TABLE II. Center-of-mass differential cross sections for the ${}^6\text{Li}(p, {}^3\text{He}){}^4\text{He}$ (g.s.) reaction at 45.0 MeV.

$\theta_{\text{c.m.}}$ (deg)	$\left(\frac{d\sigma}{d\Omega}\right)_{\text{c.m.}}$ ($\mu\text{b sr}^{-1}$)	Error (%)	Observed particle
20.1	102.4	5.1	${}^3\text{He}$
26.7	60.1	5.6	${}^3\text{He}$
33.3	46.9	6.2	${}^3\text{He}$
39.9	57.8	5.9	${}^3\text{He}$
46.3	86.2	5.5	${}^3\text{He}$
52.7	108.3	5.3	${}^3\text{He}$
59.1	100.6	6.1	${}^3\text{He}$
63.1	89.6	5.4	α
65.3	85.6	5.3	${}^3\text{He}$
68.2	73.0	5.6	α
71.3	64.6	5.5	${}^3\text{He}$
73.5	55.0	5.7	α
77.3	45.0	5.3	${}^3\text{He}$
79.0	41.5	5.4	α
83.1	31.0	5.3	${}^3\text{He}$
84.8	29.1	5.4	α
88.8	35.9	6.1	${}^3\text{He}$
90.7	36.0	5.4	α
94.3	48.8	5.3	${}^3\text{He}$
96.9	58.6	5.4	α
99.7	66.3	5.4	${}^3\text{He}$
103.2	101.2	5.5	α
109.6	139.8	5.4	α
110.0	145.5	5.5	${}^3\text{He}$
116.3	165.3	5.4	α
123.0	164.4	6.0	α
129.9	153.4	5.5	α
136.9	124.9	5.7	α
143.9	136.3	5.4	α
151.0	208.7	5.6	α
158.2	331.6	5.7	α

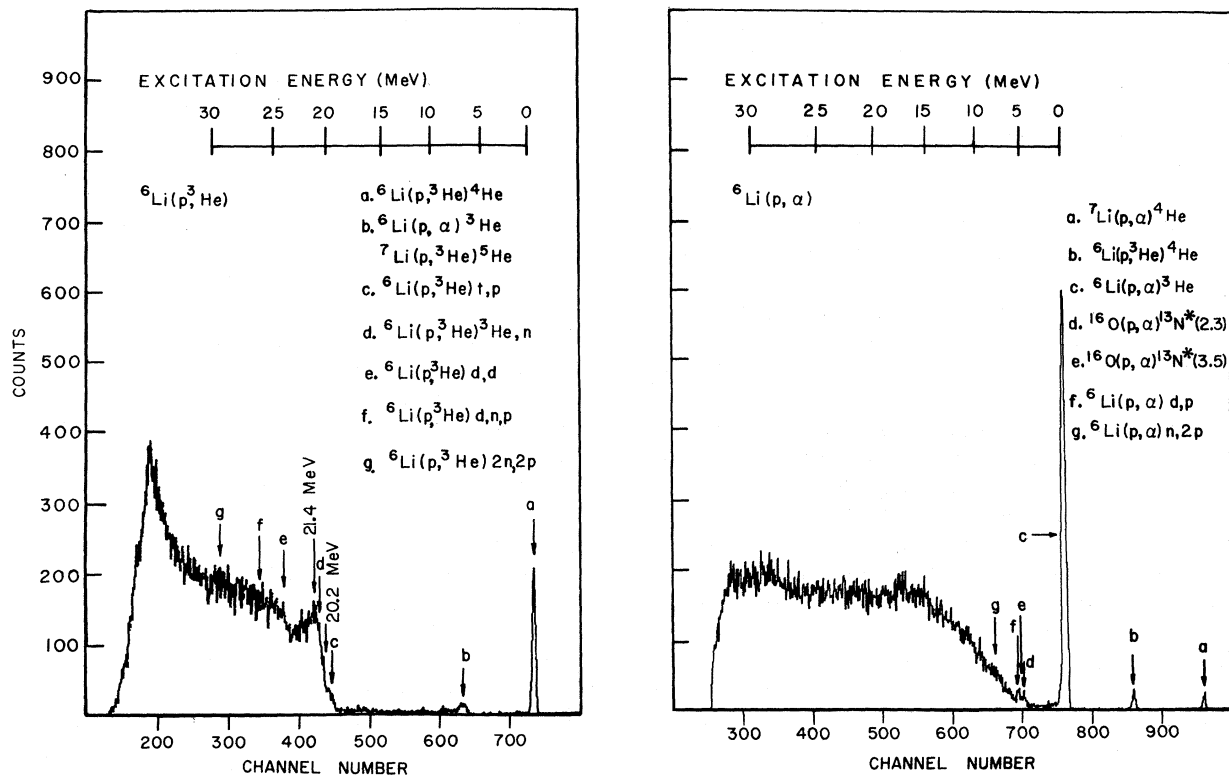


FIG. 2. Energy spectra of the ${}^6\text{Li}(p, {}^3\text{He})$ and ${}^6\text{Li}(p, \alpha)$ reactions at 15.0 (lab) using 45.0-MeV protons.

of-mass angular distribution for this reaction is shown in Fig. 1. The backward angle part of the angular distribution was obtained by observing the α particles emitted in the forward hemisphere.

The center-of-mass differential cross sections and associated relative errors are given in Table II. The relative errors were obtained from the statistical error in the number of counts, the un-

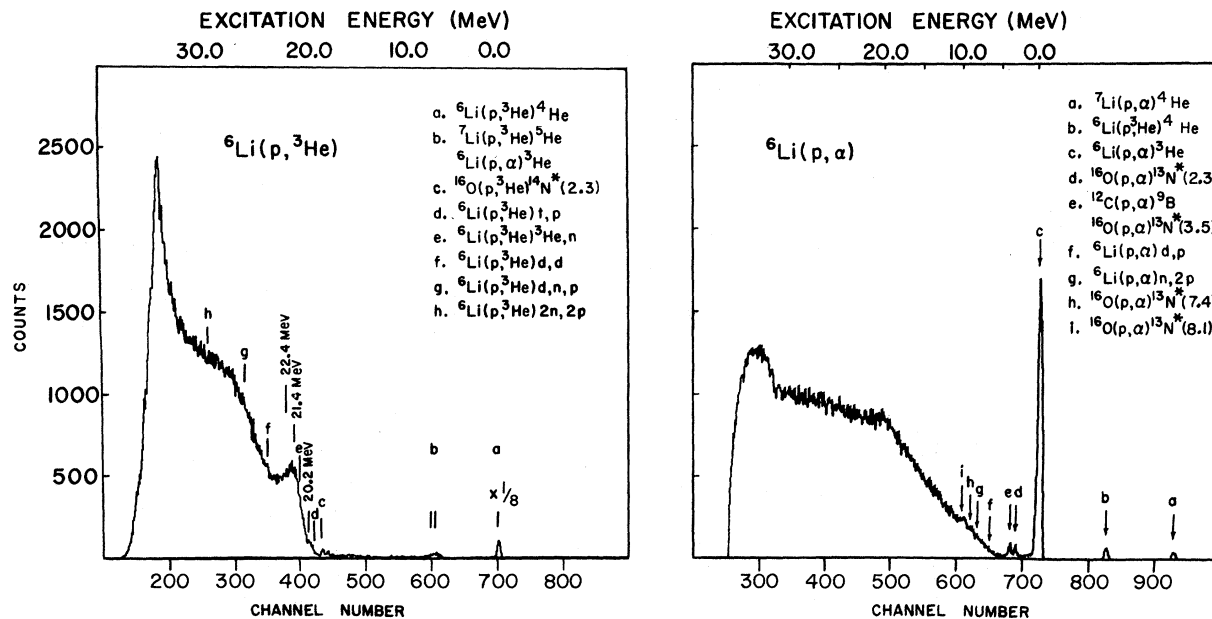


FIG. 3. Energy spectra of the ${}^6\text{Li}(p, {}^3\text{He})$ and ${}^6\text{Li}(p, \alpha)$ reactions at 25.0 (lab) using 45.0-MeV protons.

certainty in the dead-time correction, and the uncertainty in the relative normalization of the data taken with different targets. In addition there was an uncertainty in the setting of the detector angles ($\pm 0.1^\circ$) and an uncertainty in the energy of the incident proton beam (± 150 keV) for the various series of measurements. The uncertainty in the beam collection and charge integration was estimated to be 1%, while the uncertainty in the determination of the solid angle was 1.5%. The error due to target nonuniformity and thickness determination was approximately 10%. Thus, the uncertainty in the absolute scale of measurements is estimated to be 10%.

The small number of other ^3He - and α -particle peaks appearing in the spectra were identified using two methods: (1) the kinematic energy change of the peaks with angle, and (2) direct comparison of the spectra with those obtained by bombarding targets that contained C, N, and O, but no Li. The main contaminants were ^7Li present in the target material and ^{16}O introduced during the fabrication and handling of the target foil. Representative spectra obtained at 15.0, 25.0, 39.4, and 60.0° (lab) are shown in Figs. 2-5. In the figures, the

^3He spectra are shown on the left side while the α -particle spectra are shown on the right side. The uncertainty in the energy calibration of the spectra was about ± 150 keV. The figures contain a listing of the various peaks identified and the various breakup thresholds. Note that some α -particle counts were inadvertently introduced in the ^3He spectra due to particle misidentification. The ^3He spectra show peaks due to the 20.2-MeV (0^+ , $T=0$), the 21.4-MeV (1^- , $T=0$), and possibly the 22.4-MeV (2^- , $T=0$) excited states of ^4He .¹⁴ The differential cross sections for the $^6\text{Li}(p, ^3\text{He})$ - $^4\text{He}(20.2\text{-MeV})$ reaction were extracted from the ^3He spectra by means of a peak-fitting routine.

The center-of-mass angular distribution for this reaction is shown in Fig. 6. The data points at the extreme forward angles were obtained by Cerny, Detraz, and Pehl¹⁵ at 43.7 MeV. The center-of-mass differential cross sections are given in Table III together with the statistical errors.

Analyses of electron scattering experiments have shown¹⁶ that ^9Li has a large root-mean-square charge radius and a very diffuse surface as compared to other p -shell nuclei. These facts along with the results of variational calculations¹⁷ pro-

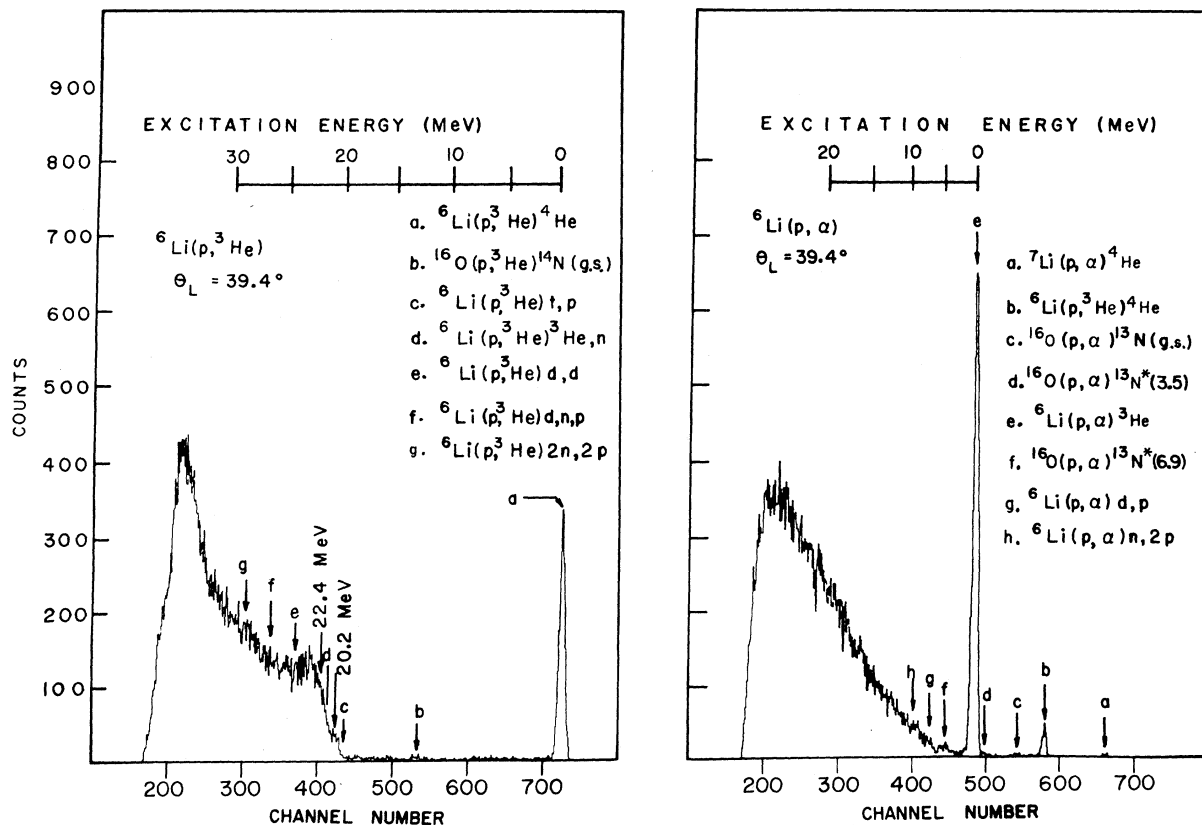


FIG. 4. Energy spectra of the $^6\text{Li}(p, ^3\text{He})$ and $^6\text{Li}(p, \alpha)$ reactions at 39.4 (lab) using 45.0-MeV protons.

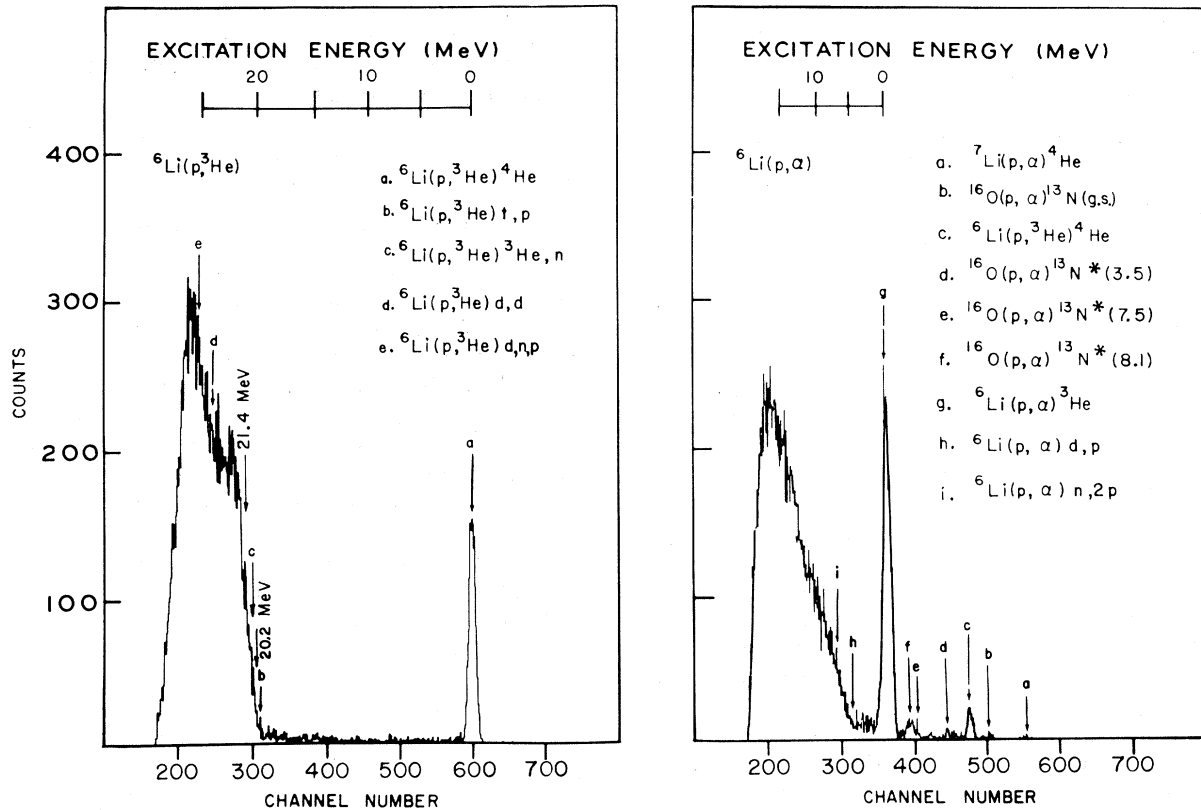


FIG. 5. Energy spectra of the ${}^6\text{Li}(p, {}^3\text{He})$ and ${}^6\text{Li}(p, \alpha)$ reactions at 60.0 (lab) using 45.0-MeV protons.

vide supporting evidence for a weakly bound (B.E. = 1.47 MeV) α - d cluster configuration for the ground state of ${}^6\text{Li}$. The angular distribution for the ${}^6\text{Li}(p, {}^3\text{He}){}^4\text{He}(\text{g.s.})$ reaction shows strong back-

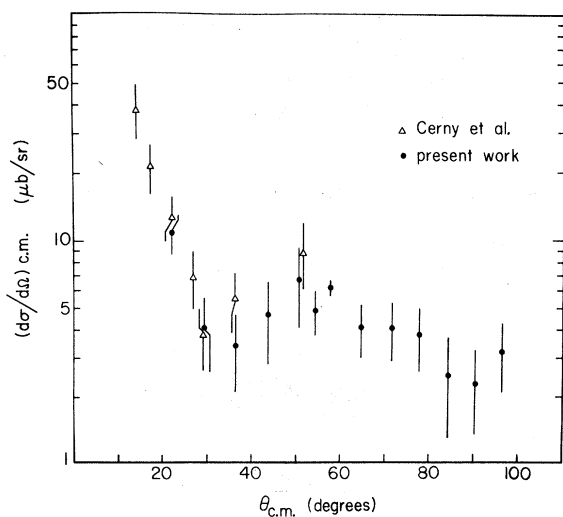


FIG. 6. Center-of-mass angular distributions for the ${}^6\text{Li}(p, {}^3\text{He}){}^4\text{He}(20.2\text{-MeV})$ reaction at 45.0 MeV. Also included in the figure are data obtained by Cerny, Detraz, and Pehl at 43.7 MeV (Ref. 15).

ward peaking. In a direct-reaction framework several processes may contribute to the particular final state; e.g., the pickup of a n - p pair from ${}^6\text{Li}$ by the incident proton; or the heavy-particle knockout of an α cluster together with capture of the incident proton by the two remaining nucleons. Apparently, in the ${}^6\text{Li}(p, {}^3\text{He}){}^4\text{He}(\text{g.s.})$ reaction the latter process dominates, which is consistent with the above observation.

One can also notice a strong similarity between the angular distributions in the forward hemisphere for the ${}^6\text{Li}(p, {}^3\text{He}){}^4\text{He}(\text{g.s.})$ and ${}^6\text{Li}(p, {}^3\text{He}){}^4\text{He}(20.2\text{-MeV})$ reactions, as might be expected because both reactions involve states of the residual nucleus which are characterized by $J^\pi = 0^+$. A corresponding similarity is noticeable in a comparison of the ${}^7\text{Li}(p, \alpha){}^4\text{He}(\text{g.s.})$ reaction at 30.2 MeV¹⁸ with the ${}^7\text{Li}(p, \alpha){}^4\text{He}(20.2\text{-MeV})$ reaction at 9.0 MeV.¹⁹

In the α -particle spectra no clearly discernible structure has been observed that could be interpreted as due to $T = \frac{1}{2}$ excited states in ${}^3\text{He}$ for excitation energies up to 17.5 MeV. In order to find an upper limit for the excitation of such states in ${}^3\text{He}$ the α -particle spectra were analyzed using a computer code which automatically identifies the peaks in complex spectra.²⁰ The upper limits

TABLE III. Center-of-mass differential cross sections for the ${}^6\text{Li}(p, {}^3\text{He}){}^4\text{He}(20.2\text{-MeV})$ reaction at 45.0 MeV.

$\theta_{\text{c.m.}}$ (deg)	$\left(\frac{d\sigma}{d\Omega}\right)_{\text{c.m.}}$ ($\mu\text{b sr}^{-1}$)	Error (%)
22.0	10.9	20
29.3	4.1	36
36.5	3.4	38
43.7	4.7	40
50.7	6.7	39
54.2	4.9	22
57.7	6.2	8
64.5	4.1	27
71.2	4.1	30
77.7	3.8	33
84.1	2.5	48
90.3	2.3	42
96.3	3.2	35

which could be set on the differential cross section for the excitation of states in ${}^3\text{He}$ having a width ≤ 1 MeV are 20, 30, and $20 \mu\text{b sr}^{-1}$ at 15.0, 25.0, and 39.4° (lab), respectively. The structure in the spectra near the lower level threshold are the result of particle misidentification due to noise in the E detector. A marked feature in the α -particle spectra is the change in slope of the continuum around an excitation energy of 17.5 MeV (see Figs. 2 and 3). The spectra are a combination of three- and four-body continua due to the ${}^6\text{Li}(p, \alpha)p d$ and ${}^6\text{Li}(p, \alpha)ppn$ reactions, respectively. With 45.0-MeV incident protons, orbital angular momenta up to $l=4$ are involved in the breakup reactions. Conservation of angular momentum will cause the three- and four-body final states to consist of an intricate combination of angular momentum states between the various pairs of particles instead of a linear combination

of simple three-body and four-body phase-space distributions,¹² in which one assumes $l=0$ throughout. Thus, one cannot expect the continua to be completely structureless.

III. KINEMATICALLY COMPLETE EXPERIMENT ${}^6\text{Li}(p, \alpha d)p$

A. Experimental Arrangements and Procedure

In this part of the investigation the ${}^6\text{Li}(p, \alpha d)p$ reaction was studied at 45.0 MeV using a similar experimental setup to that described above. The α -particle detector consisted of a $600\text{-}\mu$ -thick partially depleted detector, while the deuteron $\Delta E - E$ counter telescope consisted of a $200\text{-}\mu$ -thick surface-barrier detector and a 5-mm-thick lithium-drifted silicon detector. Copper collimators (0.156 in. thick) with rectangular apertures (0.200 in. wide by 0.500 in. high) positioned 4.50 in. from the scattering-chamber center determined the solid angle subtended by each of the detectors. The α -particle detector and deuteron-detector telescope were placed at opposite sides of, and coplanar with, the incident beam. Measurements were performed with the α -particle detector set at 50° (lab), while the deuteron-detector telescope was moved from -50 to -100° (lab) in steps of 10° . Measurements were also made with the α -particle detector set at 30° (lab) and the deuteron-detector telescope at -80 and -100° (lab).

The α particles and deuterons were detected in fast-slow coincidence using a standard electronic technique based upon leading-edge timing. The timing signals were derived from pulses taken from the $600\text{-}\mu$ -thick α -particle detector and the $200\text{-}\mu$ -thick ΔE detector. The time resolution was about 15 nsec FWHM so that consecutive beam bursts (35 nsec apart) were well separated. Deuteron selection was accomplished with a particle

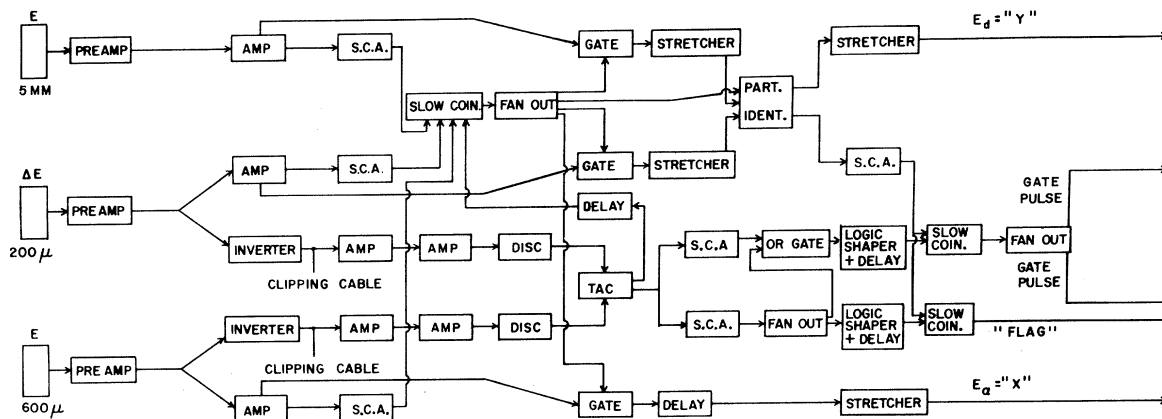


FIG. 7. Diagram of electronics used in coincidence measurements of deuterons and α particles from the ${}^6\text{Li}(p, \alpha d)p$ reaction.

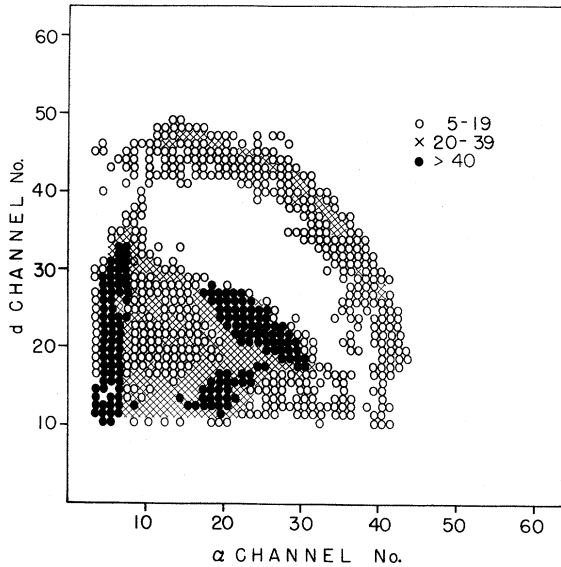


FIG. 8. α particle vs deuteron energy spectrum from the ${}^6\text{Li}(p, \alpha d)p$ reaction at 45.0 MeV with $\theta_\alpha = 50$ and $\theta_d = -60$ (lab).

identifier. The coincident analog signals together with the proper gating signals were fed into the ADC's of the PDP-9 computer. The real-plus-accidental- and accidental-coincidence spectra were recorded simultaneously using the PDP-9 computer with time windows of 30 nsec each. For some of the pairs of angles at which measurements were made, the real-plus-accidental-coincidence spectra were also recorded using a 4096-channel analyzer. All spectra were recorded in 64×64 arrays. After each measurement the data were stored on magnetic tape for further off-line analysis with an IBM 360-65 computer. A block diagram of the electronics is shown in Fig. 7.

Since the experimental technique permitted the detection of protons, deuterons, tritons, and ${}^3\text{He}$ particles in the α -particle detector, it was necessary to consider all possible reactions that could produce a background near or on the locus of the ${}^6\text{Li}(p, \alpha d)p$ reaction. Most of the allowed reactions have Q values that are much more negative than that of the ${}^6\text{Li}(p, \alpha d)p$ reaction ($Q = -1.47$ MeV). Therefore the kinematic loci for the ${}^6\text{Li}(p, {}^3\text{He}d)d$ and ${}^6\text{Li}(p, dd){}^3\text{He}$ reactions ($Q = -19.83$ MeV) do not interfere with the kinematic locus of interest. In addition, because deuterons with an energy greater than 12 MeV penetrated the α -particle detector, the kinematic locus from the ${}^6\text{Li}(p, dd){}^3\text{He}$ reaction was folded back from 12 MeV towards the low-energy α -particle side. The same held for the kinematic locus from the ${}^6\text{Li}(p, pd){}^4\text{He}$ reaction, which was folded back from 9 MeV towards the low-energy α -particle side. Therefore

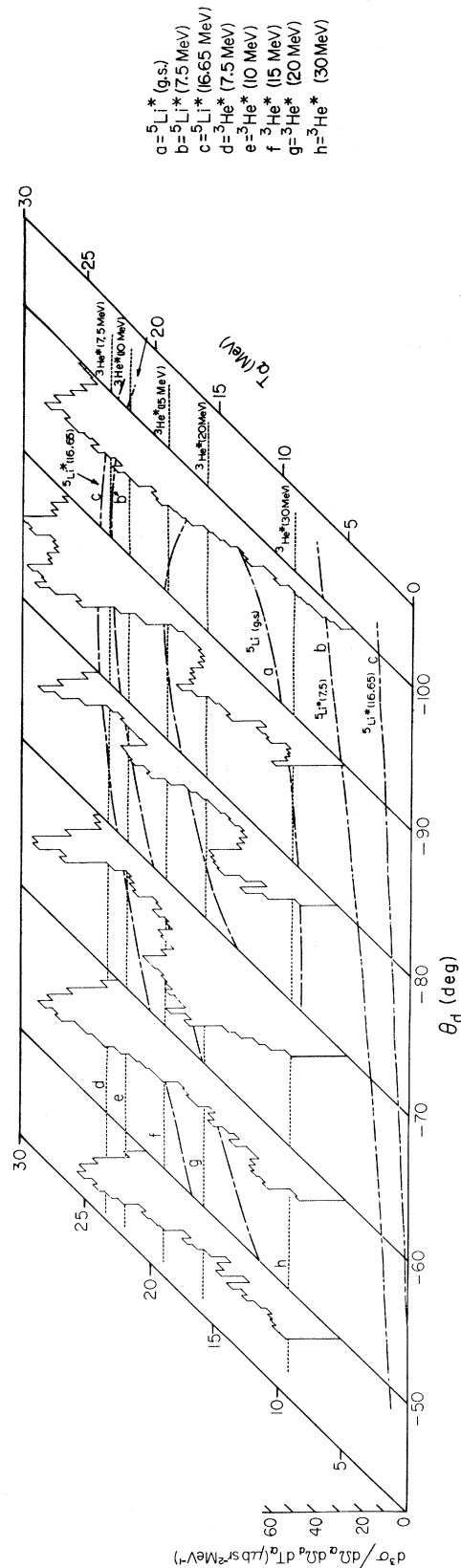


FIG. 9. α -particle-deuteron coincidence spectra from the ${}^6\text{Li}(p, \alpha d)p$ reaction at 45.0 MeV with $\theta_\alpha = 50^\circ$ and $\theta_d = -50, -60, -70, -80, -90,$ and -100° (lab) projected onto the α -particle energy axis. The dot and dash lines represent the positions of ${}^5\text{Li}$ excited states. The dotted lines correspond to constant excitation energies in ${}^3\text{He}$.

this locus crossed the kinematic locus of interest at some angle pairs.

The pairs of angles selected minimized possible enhancements due to quasifree scattering processes and due to α -particle-deuteron final-state interactions corresponding to the known excited states in ${}^6\text{Li}$. However, the presence of enhancements on the kinematical loci of the ${}^6\text{Li}(p, \alpha d)p$ reaction due to a proton- α -particle final-state interaction could not be prevented.

B. Results and Discussion

An E_α versus E_d spectrum at $\theta_\alpha = 50^\circ$ and $\theta_d = -60^\circ$ after subtraction of accidental coincidences is shown in Fig. 8. The upper band in the spectrum is due to the ${}^6\text{Li}(p, \alpha d)p$ reaction, while the lower band is due to the ${}^6\text{Li}(p, {}^3\text{He}d)d$ reaction. The α - d coincidence spectra, projected on the α -particle energy axis, for the six deuteron detector angles $-50, -60, -70, -80, -90,$ and -100° and with the α -particle detector at 50° are shown in Fig. 9. The dotted and dashed lines represent the positions of the ground, first, and second excited states in ${}^5\text{Li}$. The broken lines represent contours of constant excitation in ${}^3\text{He}$, from 7.5 MeV at the top of the figure to 30 MeV at the bottom. In these projections the energy region of greatest interest in ${}^3\text{He}$, namely, up to about 20-MeV excitation, occurs towards the high-energy end of the spectra. Any enhancement due to a p - d final-state interaction is obscured by the p - α final-state interaction

and/or a phase-space enhancement. The spectra show a strong p - α final-state interaction corresponding to the ground state of ${}^5\text{Li}$. No other strong enhancement is visible in these projections. The α - d coincidence spectra projected on the α -particle energy axis for $\theta_d = -80$ and -100° and $\theta_\alpha = 30^\circ$ are shown in Fig. 10. Similar remarks can be made with regard to the latter two spectra.

The α - d coincidence spectra projected on the deuteron energy axis are shown in Figs. 11 and 12. The spectra show that the threefold differential cross section is to a large extent due to a p - α final-state interaction. Sequential decay through the ground state of ${}^5\text{Li}$ is responsible for the prominent peaks present in the measured coincidence spectra. Very little enhancement due to sequential decay through the first excited state of ${}^5\text{Li}$ can be expected, because of the large width of this state ($\Gamma = 3$ –5 MeV). There is little evidence in the coincidence spectra for enhancements due to the second excited state in ${}^5\text{Li}$, presumably because this state has predominantly a $d + {}^3\text{He}$ cluster structure.²¹ It should be pointed out, however, that the 16.65-MeV ($\frac{3}{2}^+, T = \frac{1}{2}$) second excited state in ${}^5\text{Li}$ is responsible for a pronounced fluctuation in the excitation functions for $p + {}^4\text{He}$ elastic scattering around an incident proton energy of 23 MeV.²² The α - d coincidence spectra show no enhancement, which would indicate a relatively narrow p - d final-state interaction corresponding to a $T = \frac{1}{2}$ resonance in ${}^3\text{He}$ for the range of excitation energies

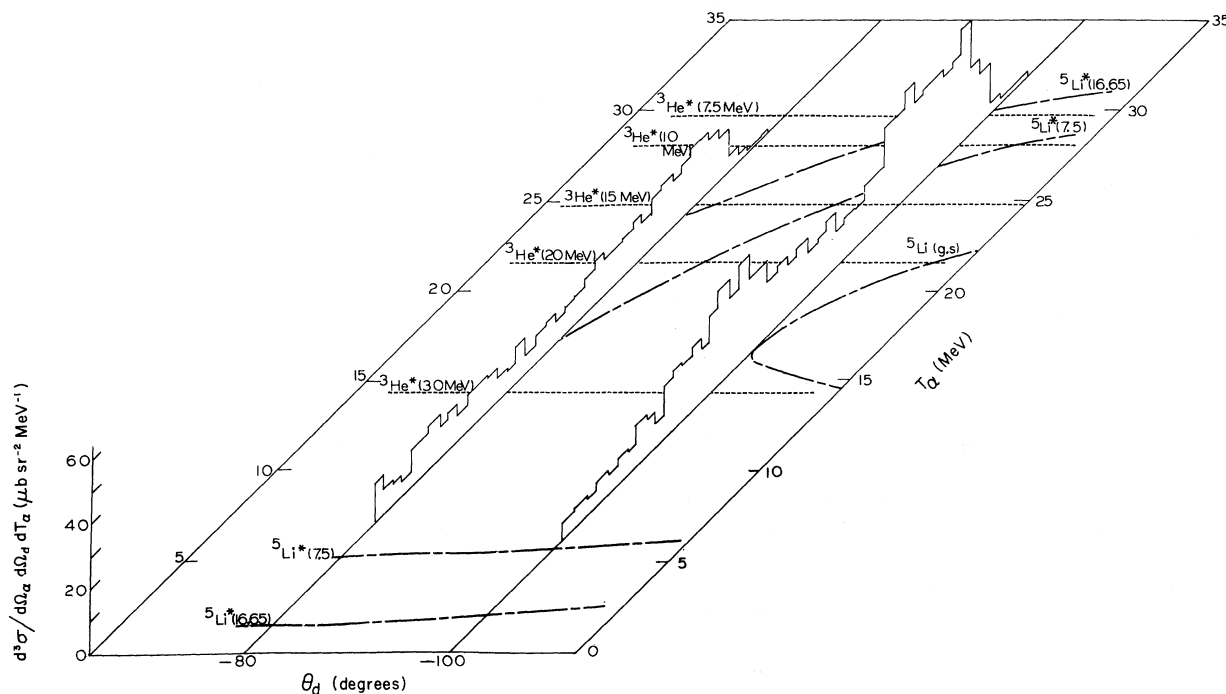


FIG. 10. The legend is the same as for Fig. 9, except $\theta_\alpha = 30^\circ$ and $\theta_d = -80$ and -100° (lab).

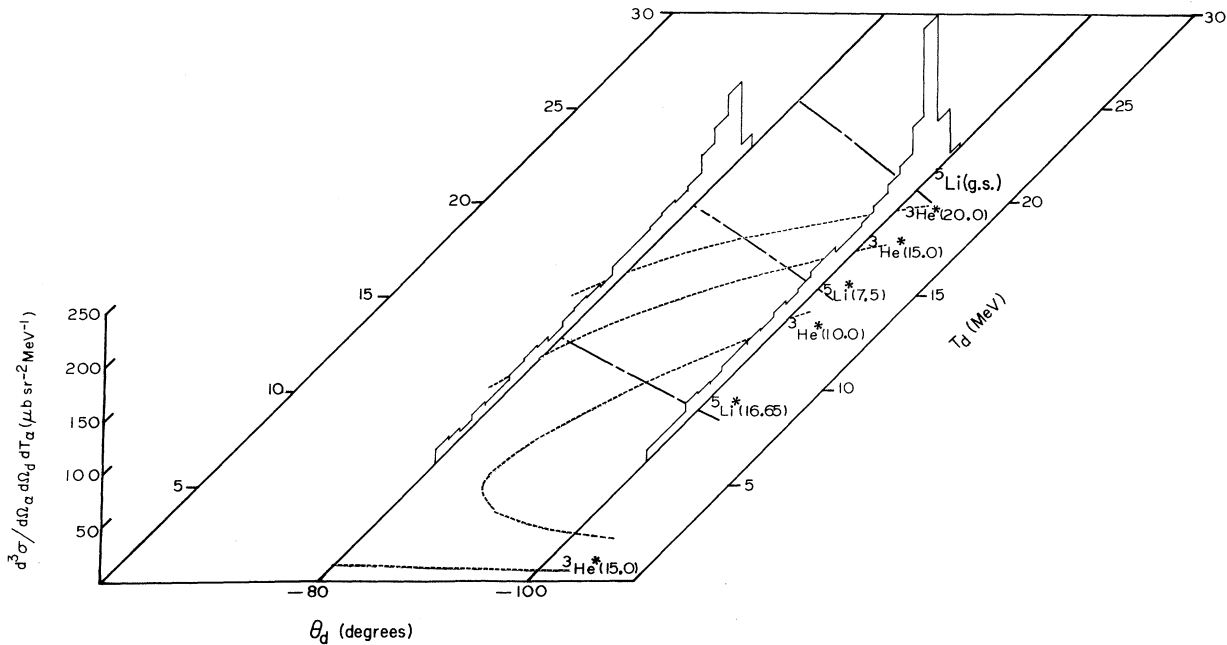


FIG. 12. The legend is the same as for Fig. 11, except $\theta_\alpha = 30^\circ$ and $\theta_d = -80$ and -100° (lab).

for a broad 4P and 2P resonance. This evidence of a 2P resonance is in disagreement with the results of the phase-shift analysis. Because of its width a 4P resonance in the nucleon-deuteron system will go unnoticed in any coincidence measurement such as of the $^6\text{Li}(p, \alpha d)p$ reaction. Studies of the charge-exchange reactions $^3\text{He}(p, n)^3p$, $^3\text{H}(p, n)^2n$, and $^3\text{He}(\pi^-, \pi^+)^3n$, in which only one of the four particles in the final state is observed, cannot unambiguously distinguish between angular

momentum effects which modify the phase-space distribution and possible broad resonances in the three-nucleon system. Thus a phase-shift analysis in terms of complex split-phase shifts of elastic nucleon-deuteron scattering and possibly a study of the energy dependence of the capture cross sections of protons or neutrons by deuterons appear to be the most promising means to learn about $T = \frac{1}{2}$ and $T = \frac{3}{2}$ resonances in the three-nucleon system.

†Work supported in part by the Atomic Energy Control Board of Canada.

*Present address: Department of Physics, University of Alberta, Edmonton, Canada.

¹V. Ajdacić, M. Cerineo, B. Lalović, G. Paić, I. Šlaus, and P. Tomas, *Phys. Rev. Letters* **14**, 444 (1965).

²C. C. Kim, S. M. Bunch, D. W. Devins, and H. H. Forster, *Phys. Letters* **22**, 314 (1966).

³H. H. Forster, J. Hokinian, and C. C. Kim, in *Nuclear Physics: An International Conference*, edited by R. L. Zucker, C. D. Goodman, P. H. Stelson, and A. Zucker (Academic Press Inc., New York, 1967), p. 1025.

⁴L. E. Williams, C. J. Batty, B. E. Bonner, C. Tscharlär, H. C. Benöhr, and A. S. Clough, *Phys. Rev. Letters* **23**, 1181 (1969).

⁵J. Sperinde, D. Frederickson, R. Hinkins, V. Perez-Mendez, and B. Smith, *Phys. Letters* **32B**, 185 (1970).

⁶G. G. Ohlsen, R. H. Stokes, and P. G. Young, *Phys. Rev.* **176**, 1163 (1968).

⁷A. I. Baz', V. I. Gol'danskii, and Ya. B. Zel'dovich, *Usp. Fiz. Nauk* **85**, 445 (1965) [transl.: *Soviet Phys.*—

Usp. **8**, 177 (1965)].

⁸W. T. H. van Oers and J. D. Seagrave, *Phys. Letters* **24B**, 562 (1967); J. D. Seagrave and W. T. H. van Oers, in *Few-Body Problems, Light Nuclei, and Nuclear Interactions*, edited by G. Paić and I. Šlaus (Gordon and Breach, Science Publishers, Inc., New York, 1968), p. 873.

⁹E. P. Wigner, *Phys. Rev.* **98**, 145 (1955).

¹⁰W. Bartolini, R. E. Donaldson, and D. J. Groves, *Phys. Rev.* **174**, 313 (1968).

¹¹P. F. Donovan, *Rev. Mod. Phys.* **37**, 501 (1965).

¹²B. V. Rybakov, V. A. Sidorov, and N. A. Vlasov, *Nucl. Phys.* **23**, 491 (1961); W. T. H. van Oers and K. W. Brockman, Jr., *Nucl. Phys.* **74**, 73 (1965).

¹³K. H. Bray, K. S. Jayaraman, G. A. Moss, W. T. H. van Oers, D. O. Wells, and Y. I. Wu, to be published; Y. I. Wu, Ph.D. thesis, University of Manitoba, 1970 (unpublished).

¹⁴W. E. Meyerhof and T. A. Tombrello, *Nucl. Phys.* **A109**, 1 (1968).

¹⁵J. Cerny, C. Detraz, and R. H. Pehl, *Phys. Rev. Lett.*

ters **15**, 300 (1965).

¹⁶E. W. Schmid, Y. C. Tang, and K. Wildermuth, *Phys. Letters* **7**, 263 (1963).

¹⁷K. Wildermuth and W. McClure, in *Cluster Representations of Nuclei*, Springer Tracts in Modern Physics, edited by G. Höhler (Springer-Verlag, Berlin, Germany, 1966), Vol. 41.

¹⁸D. W. Devins, S. M. Bunch, H. H. Forster, J. Hokhikian, and C. C. Kim, *Nucl. Phys.* **A126**, 261 (1969).

¹⁹W. K. Lin, F. Scheibling, and R. W. Kavanagh, *Phys. Rev. C* **1**, 816 (1970).

²⁰T. Harper, I. Mouye, and N. C. Rasmussen, *Nucl. Instr. Methods* **67**, 125 (1969).

²¹L. D. Pearlstein, Y. C. Tang, and K. Wildermuth, *Phys. Rev.* **120**, 224 (1960); D. R. Thompson, I. Reichstein, W. McClure, and Y. C. Tang, *Phys. Rev.* **185**, 1351 (1969).

²²P. Darriulat, D. Garreta, A. Tarrats, and J. Testoni, *Nucl. Phys.* **A108**, 316 (1968); S. N. Bunker, J. M. Cameron, M. B. Epstein, G. Paić, J. R. Richardson, J. G. Rogers, P. Tomas, and J. W. Verba, *Nucl. Phys.* **A133**, 537 (1969).

²³D. K. Olsen and R. E. Brown, *Phys. Rev.* **176**, 1192 (1968).

²⁴V. Valkovic, C. Joseph, S. T. Emerson, and G. C. Phillips, *Nucl. Phys.* **A106**, 138 (1968).

²⁵A. S. Wilson, M. C. Taylor, J. C. Legg, and G. C. Phillips, *Nucl. Phys.* **A130**, 624 (1969).

²⁶D. Daronian, J. C. Faivre, D. Garreta, J. Goudergues, J. Jungerman, H. Krug, B. Mayer, A. Pages, A. Papi-neau, and J. Testoni, *Nucl. Phys.* **A104**, 111 (1967).

²⁷J. D. Seagrave, in *Three-Body Problem in Nuclear and Particle Physics*, edited by J. S. C. McKee and P. M. Rolph (North-Holland Publishing Company, Amsterdam, The Netherlands, 1970), p. 41.

²⁸W. Haeberli, in *Three-Body Problem in Nuclear and Particle Physics*, edited by J. S. C. McKee and P. M. Rolph (North-Holland Publishing Company, Amsterdam, The Netherlands, 1970), p. 188.

²⁹W. T. H. van Oers and K. W. Brockman, Jr., *Nucl. Phys.* **92**, 561 (1967).

³⁰W. Ebenhöf, A. S. Rinat-Reiner, and Y. Avishai, *Phys. Letters* **B29**, 638 (1969).

Strong-Interaction Effects in K -Mesonic Atoms*

William A. Bardeen and E. Wayne Torigoe†

Institute of Theoretical Physics, Department of Physics, Stanford University, Stanford, California 94305

(Received 13 January 1971)

The process of absorption in K -mesonic atoms is studied with special emphasis on the role of the $Y_0^*(1405)$ resonance. An effective t -matrix method is developed to incorporate the effects of the resonance. Detailed calculations of the absorption process, based on an independent-particle model of the nucleus, were made for selected nuclei. The results of these calculations are compared with available x-ray and emulsion data for moderate to heavy nuclei.

I. INTRODUCTION

While electron scattering experiments¹ and the study of muonic atoms² provide effective means of acquiring detailed information on proton distributions, simple probes of the neutron distribution have yet to be found. The scattering of hadrons off nuclei can be used to study nuclear structure and average nuclear properties, but isolation of the neutron distribution requires interpretation of many types of experimental results. In the study of pionic atoms,³ absorption of protons and neutrons may be distinguished, but the absorption requires two nucleons, resulting in a strong dependence on nuclear correlations.

Although techniques for directly measuring the entire neutron distribution in nuclei do not exist, the study of K -mesonic atoms was proposed by Wilkinson⁴ as an effective probe of nucleon densities in the nuclear periphery. Calculations by Jones⁵ indicated that the K meson would be large-

ly trapped in circular orbits during the electronic cascade prior to absorption in the nuclear surface. On the basis of the position of the K -meson-proton overlap for these orbits, as shown for a typical case in Fig. 1, the absorption of K mesons is expected to take place in the low-density region at the nuclear surface. Unlike the absorption in π -mesonic atoms, absorption on single nucleons is possible via the open inelastic channels

$$\begin{aligned} K^- + p &\rightarrow \Sigma^+ + \pi^-, \Sigma^0 + \pi^0, \Sigma^- + \pi^+, \Lambda + \pi^0, \\ K^- + n &\rightarrow \Sigma^0 + \pi^-, \Sigma^- + \pi^0, \Lambda + \pi^-, \end{aligned} \quad (1)$$

which release sufficient energy to overcome even the largest possible binding energies of the nucleon and K meson. Thus, with appropriate information on the rates for these reactions, the nucleon densities in the nuclear periphery, to a first approximation, are directly given by measurements of absorption rates in K -mesonic atoms. Following this initial description of the absorption pro-